
Boundary Layer Flow and Heat Transfer of Micropolar Fluid over a Vertical Exponentially Stretched Cylinder

Abdul Rehman¹, Razmak Bazai¹, Sallahuddin Achakzai¹, Saleem Iqbal¹, Muhammad Naseer²

¹Department of Mathematics, University of Balochistan, Quetta, Pakistan

²Department of Mathematics, Quaid-i-Azam University, Islamabad, Pakistan

Email Address:

rehman_maths@hotmail.com (A. Rehman), razmakkar939@gmail.com (R. Bazai), skachakzai33@gmail.com (S. Achakzai), saleemiqbal81@yahoo.com (S. Iqbal), naseermaths@yahoo.com (M. Naseer)

To cite this article:

Abdul Rehman, Razmak Bazai, Sallahuddin Achakzai, Saleem Iqbal, Muhammad Naseer. Boundary Layer Flow and Heat Transfer of Micropolar Fluid over a Vertical Exponentially Stretched Cylinder. *Applied and Computational Mathematics*. Vol. 4, No. 6, 2015, pp. 424-430. doi: 10.11648/j.acm.20150406.15

Abstract: The current paper offers an analysis of the steady boundary layer flow and heat transfer of a non-Newtonian micropolar fluid flowing through a vertical exponentially stretching cylinder along its axial axis. The obtained system of nonlinear partial differential equations along with the appropriate boundary conditions is abridged to dimensionless form by means of the boundary layer estimates and a suitable similarity transformation. The subsequent nonlinear coupled system of ordinary differential equations subject to the appropriate boundary conditions is solved numerically with the help of Keller-box method. The effects of the involved parameters are presented through graphs. The allied physical features for the flow and heat transfer characteristics that is the skinfriction coefficient and Nusselt numbers are presented for different parameters.

Keywords: Boundary Layer Flow, Vertical Cylinder, Micropolar Fluid, Heat Dissipation, Keller-Box Method

1. Introduction

The fundamental idea about the micropolar fluid was given by Egingen [1] because the Newtonian fluid theory does not exhibit all the properties of some complex nature fluids like liquid crystals, suspensions containing micro size particles, lubricants are a few particular examples of micropolar fluids. The idea was to make use of the law of conservation of angular momentum along with the conservation of mass and linear momentum. In recent years many researchers have discussed the study of micropolar fluids for different geometries and various situations due to its real world applications. Rosali et al [2] have prescribed the behavior of micropolar fluids flowing towards a permeable stretching sheet immersed in a porous medium and the fluid flow was assumed to be effected via suction through the surface of the sheet. The problem of heat generation or absorption effects over the heat transfer and stagnation-point fluid flow of a micropolar fluid flowing over a stretching surface is presented by Attia [3]. His effort indicated that the micropolar fluid parameter effects over flow and heat transfer depends upon the stretching velocity magnitude. Further, Nazar et al [4] have analyzed the problem of unsteady, boundary layer,

incompressible flow of a micropolar fluid over a stretching sheet. Moreover, Nadeem et al [5] have provided the analytical analysis of the problem of axisymmetric stagnation flow of a micropolar nanofluid in a moving cylinder. The fluid flow was assumed to be through the annular region between the two concentric cylinders. In another work, Nadeem et al [6] have inspected the influence of micropolar fluid flow in a vertical annulus. Few other interesting works concerning the micropolar fluid flow for different geometries are referred in [7-10].

Fluid flow over a cylinder that is stretched linearly along its axial direction has gained much attention in recent years. Bachok and Ishak [11] have tackled the problem of laminar flow of an incompressible viscous fluid flow over a stretching cylinder with prescribed surface heat flux. In a fresh attempt, Gang et al [12] have debated the problem of unsteady viscous fluid flowing over a stretching cylinder. In another work, Fag and Yao [13] have discussed the viscous swirling flow over a stretching cylinder. Recently, Wang [14] has communicated the influence of natural convection heat transfer over a vertical stretching cylinder. Few pertinent works concerning the boundary layer flow over stretching surfaces are cited in [15-21]. The determination of the contemporary effort is to

provide a numerical solution for the flow of a non-Newtonian micropolar fluid flowing over a vertical cylinder that is stretched exponentially along the axial direction taking into account the dissipation effects. The numerical solutions are computed by applying the second order finite difference scheme, known as the Keller-box technique. The influence of involved parameters is graphed in the results and discussion section. The important physical features associated with the problem like the skinfriction coefficient and the local Nusselt numbers are discussed at the end.

2. Formulation

Consider the problem of mixed convection boundary layer flow of a viscous fluid flowing over a vertical circular cylinder of radius a . The cylinder is assumed to be stretching exponentially along the axial direction with velocity U_w . The temperature at the surface of the cylinder is assumed to be a constant T_w and the uniform ambient temperature is taken to be T_∞ such that the quantity $T_w - T_\infty > 0$ in case of the assisting flow, while $T_w - T_\infty < 0$ in case of the opposing flow, respectively. Under these assumptions the boundary layer equations of motion and heat transfer are

$$u_r + \frac{u}{r} + w_z = 0, \tag{1}$$

$$uw_r + ww_z = -\frac{1}{\rho} \frac{\partial p}{\partial z} + \nu(1 + K)(w_{rr} + \frac{1}{r} w_r) + \nu K(\frac{N}{r} + N_r) + g\beta(T - T_\infty), \tag{2}$$

$$uN_r + wN_z = \nu\Lambda(N_{rr} + \frac{1}{r} N_r - \frac{N}{r^2}) - \frac{\gamma K}{j}(w_r + 2N), \tag{3}$$

$$uT_r + wT_z = \alpha(T_{rr} + \frac{1}{r} T_r) + \frac{\nu}{c_p} w_r^2, \tag{4}$$

where the velocity components along the (r, z) axes are (u, w) , ρ is density, ν is the kinematic viscosity, p is pressure, g is the gravitational acceleration along the z - direction, β is the coefficient of thermal expansion, N is the angular velocity, K is the micropolar parameter, γ is the micropolar constant, j is the microrotation density, T is the temperature, α is the thermal diffusivity and c_p is the specific heat at constant pressure. The corresponding boundary conditions for the problem are

$$u(a, z) = 0, w(a, z) = U_w, w(r, z) \rightarrow 0 \text{ as } r \rightarrow \infty, \tag{5}$$

$$N(a, x) = n(u_z - w_r)|_{r=a}, N(r, z) \rightarrow 0 \text{ as } r \rightarrow \infty, \tag{6}$$

$$T(a, z) = T_w(z), T(r, z) \rightarrow T_\infty \text{ as } r \rightarrow \infty, \tag{7}$$

where $U_w = 2ake^{z/a}$ is the fluid velocity at the surface of the cylinder.

3. Solution of the Problem

Introduce the following similarity transformations:

$$u = -ake^{z/a} \frac{f(\eta)}{\sqrt{\eta}}, w = 2ake^{z/a} f'(\eta), \tag{8}$$

$$N = ke^{z/a} \frac{M(\eta)}{\sqrt{\eta}}, \theta = \frac{T - T_\infty}{T_w - T_\infty}, \eta = \frac{r^2}{a^2}, \tag{9}$$

where the characteristic temperature difference is calculated from the relations $T_w - T_\infty = ce^{z/a}$. With the help of transformations (6) and (7), Eqs. (1) to (3) take the form

$$(1 + K)(\eta f''' + f'') + \text{Re}(ff'' - f'^2) + \frac{K}{4}M' + \text{Re}\lambda\theta = 0, \tag{10}$$

$$\eta M'' + \frac{\text{Re}}{\Lambda}(fM' - f'M) - \frac{\text{Re}}{2\Lambda\eta}fM - \frac{bK}{\Lambda}(2\eta f' + M) = 0, \tag{11}$$

$$\eta\theta'' + \theta' + \text{Re Pr}(f\theta' - f'\theta) + \text{Pr Ec}\eta f'^2 = 0, \tag{12}$$

in which $\text{Re} = aU_w / 4\nu$ is the Reynolds number, K is the micropolar parameter, $\lambda = g\beta a(T_w - T_\infty) / U_w^2$ is the natural convection parameter, and $b = a^2 / 2j$ are the micropolar coefficients, $\text{Pr} = \nu / \alpha$ is the Prandtl number and $\text{Ec} = U_w^2 / c_p(T_w - T_\infty)$ is the Eckert number. The boundary conditions in nondimensional form become

$$f(1) = 0, f'(1) = 1, f' \rightarrow 0, \text{ as } \eta \rightarrow \infty, \tag{13}$$

$$M(1) = -4nf''(1), M \rightarrow 0, \text{ as } \eta \rightarrow \infty, \tag{14}$$

$$\theta(1) = 1, \theta \rightarrow 0, \text{ as } \eta \rightarrow \infty. \tag{15}$$

The important physical quantities such as the shear stress at the surface τ_w , the skinfriction coefficient c_f , the heat flux at the surface of the cylinder q_w and the local Nusselt number Nu are

$$\tau_w = \tau_{rz}|_{r=a}, c_f \text{Re} = f''(1), \tag{16}$$

$$q_w = -k_0 T_r|_{r=a}, Nu / \text{Re} = -\theta'(1). \tag{17}$$

The solution of Eqs.(10-12) subject to the boundary conditions (13-15) is obtained through the highly

sufficient second order numerical scheme called the Keller-box technique. To develop the technique, the system of differential equations (10–12) along with the boundary conditions (13–15) is converted into a first order differential system by choosing

$$F_1 = f', \quad F_2 = F_1', \quad F_3 = M', \quad F_4 = \theta', \quad (18)$$

the resulting system can be stated now as

$$(1 + K)(\eta F_2' + F_2) + \text{Re}(f F_2 - F_1^2) + \frac{K}{4} F_3 + \text{Re} \lambda \theta = 0 \quad (19)$$

$$\eta F_3' + \frac{\text{Re}}{\Lambda}(f F_3 - F_1 M) - \frac{\text{Re}}{2\Lambda\eta} f M - \frac{bK}{\Lambda}(2\eta F_1 + M) = 0, \quad (20)$$

$$\eta F_4' + F_4 + \text{Re Pr}(f F_4 - F_1 \theta) + \text{Pr Ec} \eta F_2^2 = 0, \quad (21)$$

with the boundary conditions

$$f(1) = 0, \quad u(1) = 1, \quad u \rightarrow 0, \quad \text{as } \eta \rightarrow \infty, \quad (22)$$

$$M(1) = -4\eta f''(1), \quad \theta \rightarrow 0, \quad \text{as } \eta \rightarrow \infty, \quad (23)$$

$$\theta(1) = 1, \quad \theta \rightarrow 0, \quad \text{as } \eta \rightarrow \infty, \quad (24)$$

Further details of the numeric solution can be found in references [22-25]. The detailed discussion about the obtained numeric solutions is presented in the next section.

4. Results and Discussion

The present work is an effort to provide a numerical scheme that gives the solution of the problem of natural convection boundary layer flow of a non-Newtonian micropolar fluid flowing over a vertical cylinder that is stretched exponentially along its axial axis. The numerical solutions of the problem are computed using the second order implicit finite difference scheme called the Keller-box method. The influence of the involved parameters is presented both graphically and in tabulated form in this section. The solutions are computed for both strong concentration ($n = 1/2$) and weak concentration ($n = 0$) of the angular velocity at the surface of the stretching cylinder. *Fig.1* displays the influence of velocity profile f' for different combinations of Reynolds numbers Re and the micropolar parameter K , for fixed values of the other parameters. The solutions in *Fig.1* are curved for strong concentration case and the range of Reynolds numbers is chosen up to $\text{Re} = 20000$ (such high values of Re corresponds to turbulent flows). From *Fig.1*, it clicks that with the increase in Re the velocity profile decreases whereas with increase in K the velocity profile increases. *Fig.2* is graphed to observe the impact of natural convection parameter λ and the Eckert number Ec . From *Fig.2* it is observed that with increase in both λ and Ec

the velocity profile increases. This strengthen the observation that enhanced natural convection parameter λ requires higher density difference in fluid that in return requests increase in fluid velocity. It is also noticed from *Fig.2* that the influence of natural convection parameter is more significant for higher values of Eckert numbers. *Fig.3* conveys the behavior of velocity profile f' plotted for different values of micropolar parameter K for both the strong and weak concentration cases. From *Fig.3* it is noticed that the velocity profile f' has larger values for strong concentration as compared with the weak concentration situation. The pattern adopted by the non-dimensional angular velocity profile $M(\eta)$ is presented for strong concentration in *Figs.(4–5)* for different combinations of involved parameters. *Fig.4* gives the impact of micropolar parameter K and natural convection parameter λ over the micropolar velocity profile M . From *Fig.4* it is noted that with increase in both K and λ the micropolar velocity profile M decreases. *Fig.5* predicts the impact of micropolar coefficient Λ and the Reynolds numbers Re for the micropolar velocity M . From *Fig.5* it is witnessed that with increase in the micropolar velocity profile increases, whereas with increase in Re the micropolar velocity profile M decreases. The imprint of micropolar parameter K , Eckert numbers Ec and Prandtl numbers Pr over the non-dimensional micropolar velocity function is portrayed in *Figs.(6–7)* for the weak concentration case. *Fig.6* inculcates the imprint of micropolar velocity for different pairs of the micropolar parameter K and the Eckert numbers Ec . From *Fig.6* it is observed that with increase in both K and λ the angular velocity profile decreases. It is also noticed from *Fig.6* that the influence of K is significant for large values of the Eckert numbers Ec . *Fig.7* is sketched to observe the impact of Prandtl numbers Pr up to $\text{Pr} = 50$ over the micropolar velocity profile Λ . From *Fig.7* it is observed that with increase in Pr the angular velocity profile decreases. The behavior of non-dimensional velocity profile is plotted in *Figs.(8–9)* for different combinations of Prandtl numbers, Eckert numbers, Reynolds numbers and micropolar parameter. *Fig.8* contains the curves predicting the influence of Pr and Ec over the temperature profile θ . From *Fig.8* it is noted that with increase in both Pr and Ec the temperature profile decreases. *Fig.9* shows the impact of K and Re over the temperature profile θ for Reynolds numbers up to $\text{Re} = 5000$. From *Fig.9* it is observed that with increase in both K and Re the temperature profile and the thermal boundary layer thickness decays. The behavior of skinfriction coefficient c_f for different Prandtl numbers and Reynolds numbers is shown in *Fig.10* plotted against micropolar parameter K . From the observed graph it is noted that with increase in all Re, Pr and K the skinfriction coefficient

increases. The pattern adopted by the local Nusselt numbers Nu for different Eckert numbers and Reynolds numbers curved against Prandtl numbers is presented in Fig.11. From Fig.11 it is observed that with increase in all the Ec, Pr and Re the local Nusselt numbers increases. Figs.(12–13) shows the streamlines for the fluid flow sketched in the (r, z) plane graphed for different K . The decaying pattern observed is slower for small values of K .

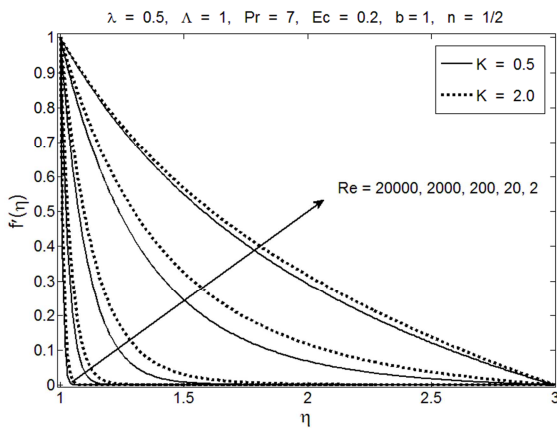


Fig. 1. Influence of Reynolds numbers Re over velocity profile f' for different K .

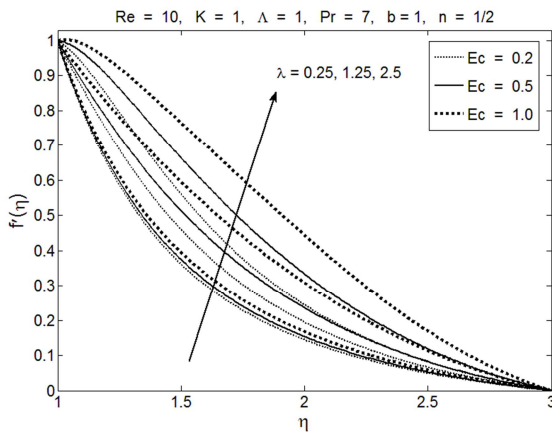


Fig. 2. Influence of natural convection parameter λ over velocity profile f' for different Ec .

The behavior of boundary derivatives for velocity, microrotation and temperature profiles is presented in Tables.(1–3). The values are computed at the surface of the stretching cylinder. Table.1 contains the values of the boundary derivatives for velocity profile that corresponds to the shear stress at the surface of the cylinder τ_w . From Table.1 it is noticed that with increase in the shear stress at the surface decreases, whereas with increase in Reynolds numbers shear stress increases. The computed vales of shear stress are larger for strong concentration as compared with the weak concentration situation. Table.2 is prepared for the boundary derivatives of the micropolar velocity profile calculated for different values of the involved parameters.

From Table.2 it is seen that with increase in K and λ the boundary derivatives increases. Table.3 shows the behavior of surface heat flux q_w computed for different values of the involved parameters. From Table.3 it is clear that with increase in K , q_w increases, whereas with increase in Ec and Pr heat flux at the surface decreases.

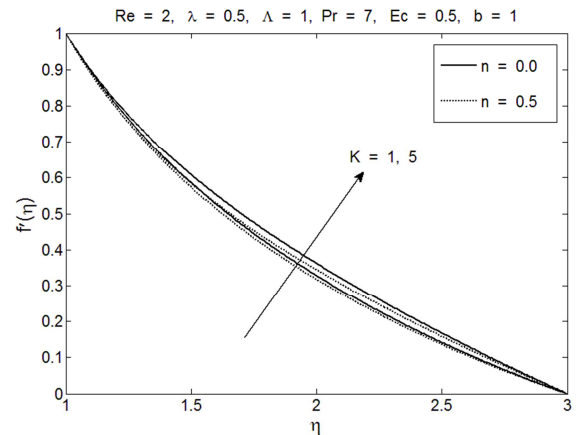


Fig. 3. Influence of micropolar parameter K over velocity profile f' for different n .

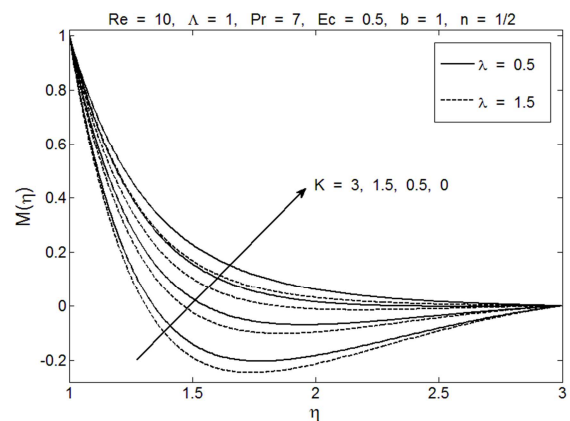


Fig. 4. Influence of micropolar parameter K over angular velocity profile M for different λ .

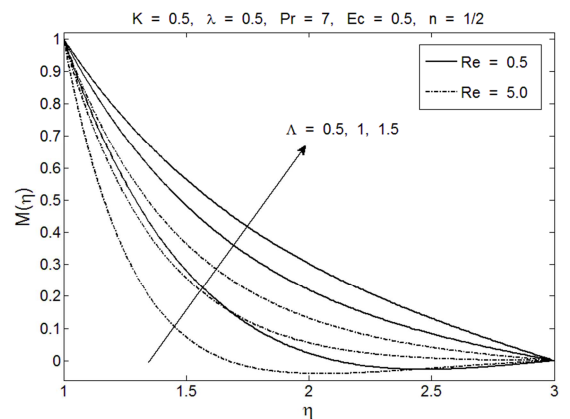


Fig. 5. Influence of micropolar parameter Λ over angular velocity profile M for different Re .

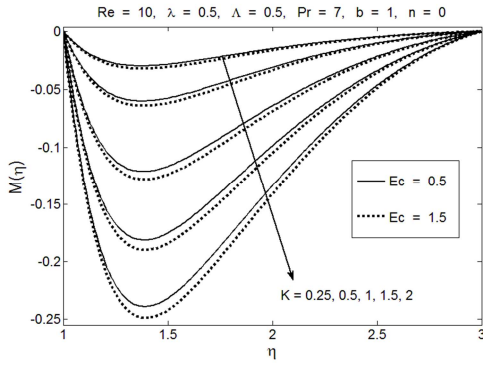


Fig. 6. Influence of micropolar parameter K over angular velocity profile M for different Ec with $n = 0$.

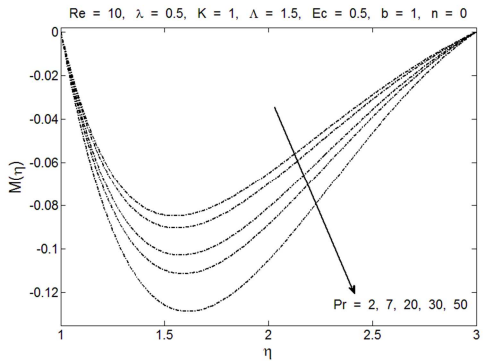


Fig. 7. Influence of micropolar parameter Pr over angular velocity profile M with $n = 0$.

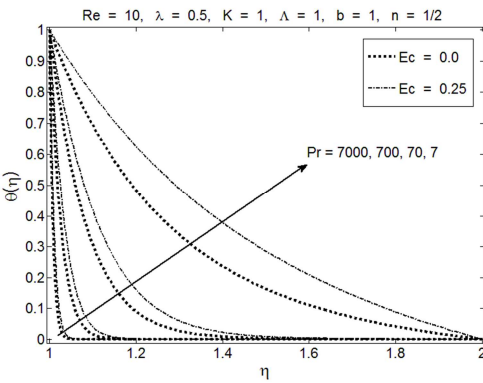


Fig. 8. Influence of Prandtl numbers Pr over temperature profile θ for different Ec

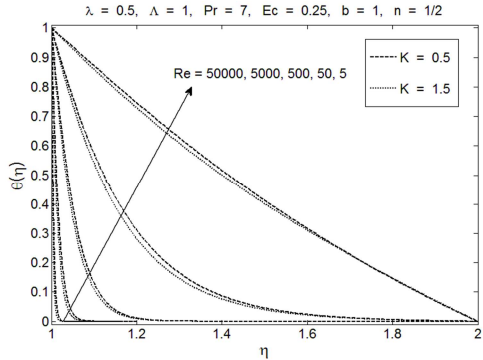


Fig. 9. Influence of Reynolds numbers Re over temperature profile θ for different K

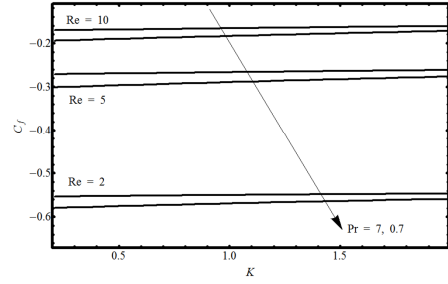


Fig. 10. Influence of Re and Pr over C_j against K for $\lambda = 0.5, \Lambda = 1, Ec = 0.5, b = 1, n = 1/2$

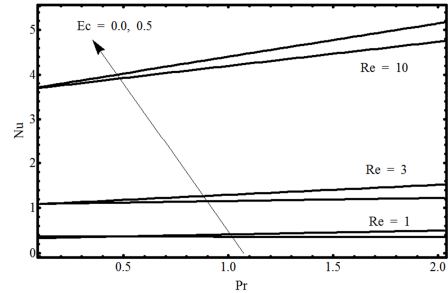


Fig. 11. Influence of Re and Ec over Nu against Pr for $\lambda = 0.5, K = 1, \Lambda = 1, b = 1, n = 1/2$

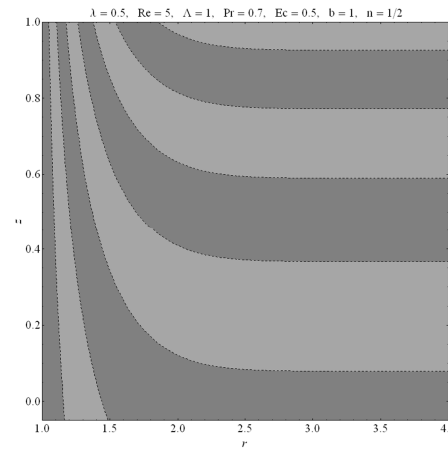


Fig. 12. Stream lines pattern for $K = 0$ in the (r, z) plane.

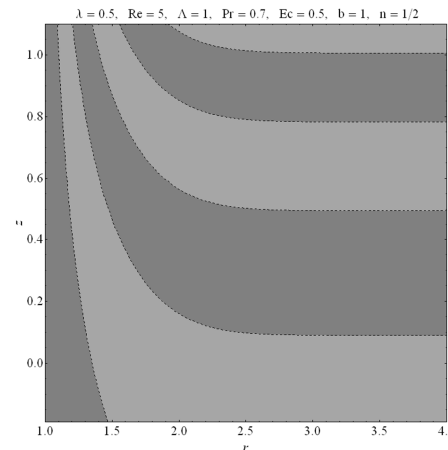


Fig. 13. Stream lines pattern for $K = 2$ in the (r, z) plane.

Table 1. Absolute values of the boundary derivatives corresponding to the behavior of shear stress at the surface of the cylinder for different values of the involved parameters when $\lambda = 0.5, \Lambda = 1, Pr = 7, Ec = 0.25, b = 1$.

| | | $f''(1)$ | | | | | | | |
|-----------|------|-------------------|--------|--------|--------|--------|--------|--------|---------|
| | | $K \backslash Re$ | 0.2 | 0.5 | 1 | 5 | 15 | 50 | 100 |
| $n = 0$ | 0.00 | 0.9516 | 1.0148 | 1.1183 | 1.8106 | 2.9470 | 5.2398 | 7.3312 | 10.2564 |
| | 0.25 | 0.9464 | 0.9980 | 1.0845 | 1.6952 | 2.7339 | 4.8464 | 6.7754 | 9.4741 |
| | 0.50 | 0.9474 | 0.9906 | 1.0645 | 1.6105 | 2.5714 | 4.5436 | 6.3475 | 8.8726 |
| | 1.00 | 0.9571 | 0.9891 | 1.0454 | 1.4943 | 2.3351 | 4.0965 | 5.7144 | 7.9828 |
| | 1.50 | 0.9702 | 0.9952 | 1.0399 | 1.4187 | 2.1686 | 3.7742 | 5.2566 | 7.3383 |
| | 2.00 | 0.9839 | 1.0040 | 1.0405 | 1.3661 | 2.0434 | 3.5263 | 4.9035 | 6.8404 |
| $n = 0.5$ | 0.00 | 0.9516 | 1.0148 | 1.1183 | 1.8106 | 2.9470 | 5.2398 | 7.3312 | 10.2564 |
| | 0.25 | 0.9682 | 1.0199 | 1.1066 | 1.7180 | 2.7573 | 4.8704 | 6.7997 | 9.4987 |
| | 0.50 | 0.9854 | 1.0290 | 1.1033 | 1.6503 | 2.6127 | 4.5859 | 6.3902 | 8.9158 |
| | 1.00 | 1.0182 | 1.0511 | 1.1083 | 1.5602 | 2.4025 | 4.1652 | 5.7836 | 8.0525 |
| | 1.50 | 1.0476 | 1.0736 | 1.1197 | 1.5026 | 2.2544 | 3.8613 | 5.3443 | 7.4263 |
| | 2.00 | 1.0737 | 1.0949 | 1.1330 | 1.4637 | 2.1431 | 3.6273 | 5.0049 | 6.9423 |

Table 2. Absolute values of the boundary derivatives of the angular velocity at the surface of the cylinder for different values of the involved parameters when $Re = 10, \Lambda = 1, Pr = 7, Ec = 0.25, b = 1$.

| | | $M'(1)$ | | | | | |
|-----------|-----|------------------------|--------|--------|--------|--------|--------|
| | | $\lambda \backslash K$ | 0.25 | 0.5 | 1 | 2 | 5 |
| $n = 0$ | 0.1 | 0.1221 | 0.2493 | 0.5104 | 1.0338 | 2.4761 | 4.4324 |
| | 0.2 | 0.1251 | 0.2542 | 0.5177 | 1.0433 | 2.4874 | 4.4434 |
| | 0.5 | 0.1324 | 0.2667 | 0.5372 | 1.0700 | 2.5202 | 4.4758 |
| | 1.0 | 0.1416 | 0.2832 | 0.5643 | 1.1095 | 2.5722 | 4.5286 |
| | 2.0 | 0.1554 | 0.3086 | 0.6078 | 1.1768 | 2.6682 | 4.6303 |
| | 5.0 | 0.1858 | 0.3648 | 0.7066 | 1.3369 | 2.9179 | 4.9122 |
| $n = 0.5$ | 0.1 | 3.1257 | 3.3433 | 3.7506 | 4.4943 | 6.3981 | 8.9317 |
| | 0.2 | 3.1662 | 3.3789 | 3.7801 | 4.5177 | 6.4154 | 8.9455 |
| | 0.5 | 3.2689 | 3.4715 | 3.8595 | 4.5833 | 6.4660 | 8.9863 |
| | 1.0 | 3.4051 | 3.5977 | 3.9721 | 4.6810 | 6.5459 | 9.0526 |
| | 2.0 | 3.6175 | 3.7981 | 4.1568 | 4.8490 | 6.6932 | 9.1799 |
| | 5.0 | 4.0974 | 4.2525 | 4.5821 | 5.2508 | 7.0752 | 9.5312 |

Table 3. Behavior of heat flux at the surface of the cylinder for different values of the involved parameters when $Re = 10, \lambda = 0.5, \Lambda = 1, b = 1, n = 1/2$.

| | | $-\Theta'(1)$ | | | | |
|-------------|-----|-------------------|--------|--------|--------|--------|
| | | $K \backslash Pr$ | 0.2 | 0.72 | 7 | 10 |
| $Ec = 0.25$ | 0.0 | 3.4686 | 3.3457 | 2.0113 | 1.4588 | 0.0701 |
| | 0.5 | 3.5528 | 3.4466 | 2.2707 | 1.7711 | 0.3452 |
| | 1.0 | 3.6083 | 3.5131 | 2.4437 | 1.9812 | 0.6321 |
| | 1.5 | 3.6478 | 3.5603 | 2.5682 | 2.1335 | 0.8447 |
| | 2.0 | 3.6775 | 3.5958 | 2.6625 | 2.2495 | 1.0095 |
| $Ec = 0.50$ | 0.0 | 3.4211 | 3.1881 | 0.7940 | 0.0702 | 0.0098 |
| | 0.5 | 3.5118 | 3.3100 | 1.1594 | 0.3452 | 0.1412 |
| | 1.0 | 3.5715 | 3.3901 | 1.4079 | 0.6321 | 0.4479 |
| | 1.5 | 3.6141 | 3.4472 | 1.5898 | 0.8448 | 0.6251 |
| | 2.0 | 3.6460 | 3.4900 | 1.7293 | 1.0096 | 0.9395 |
| | 5.0 | 3.7429 | 3.6197 | 2.1676 | 1.5371 | 1.3104 |

References

[1] A. C. Eringen, Theory of micropolar fluid, J. Math. Mech. 16 (1966) 1-18.
 [2] H. Rosali, A. Ishak, I. Pop, Micropolar fluid flow towards a stretching/shrinking sheet in a porous medium with suction, Int. Commun. Heat Mass Tran. 39 (2012) 826-829.

[3] H. A. Attia, Heat transfer in a stagnation point flow of a micropolar fluid over a stretching surface with heat generation/absorption, Tamkang J. Sci. Eng. 9 (4) (2006) 299-305.
 [4] R. Nazar, A. Ishak, I. Pop, Unsteady boundary layer flow over a stretching sheet in a micropolar fluid, Int. J. Eng. App. Sci. 4 (7) (2008) 406-410.
 [5] S. Nadeem, Abdul Rehman, K. Vajravelu, J. Lee, C. Lee, Axisymmetric stagnation flow of a micropolar nanofluid in a moving cylinder, Math. Prob. Eng. Volume 2012 (2012), Article ID 378259, 17 pages, doi:10.1155/2012/378259.
 [6] S. Nadeem, N. S. Akbar, M. Y. Malik, Exact and numerical solutions of a micropolar fluid in a vertical Annulus, Num. Meth. Part. Diff. Equ. 26 (2010) 1660-1674.
 [7] A. Ishak, R. Nazar, I. Pop, Magnetohydrodynamic stagnation point flow towards a stretching vertical sheet in a micropolar fluid, Magnetohydrodynamics, 43 (1) (2007) 83-97.
 [8] A. Ishak, R. Nazar, I. Pop, Heat transfer over a stretching surface with variable surface heat flux in micropolar fluids, Phys. Lett. A, 372 (2008) 559-561.
 [9] S. Nadeem, M. Hussain, M. Naz, MHD Stagnation flow of a micropolar fluid through porous medium, Meccanica 45 (2010) 869-880.
 [10] S. Nadeem, S. Abbasbandy, M. Hussain, Series solutions of boundary layer flow of a Micropolar fluid near the stagnation point towards a shrinking sheet, Zeitschrift fur Naturforschung. 64a (2009) 575-582.
 [11] N. Bachok, A. Ishak, Flow and heat transfer over a stretching cylinder with prescribed surface heat flux, Malaysian Journal of Mathematical Sciences 4 (2) (2010) 159-169.
 [12] T. G. Fang, J. Zhang, Y. F. Zhong, H. Tao, Unsteady viscous flow over an expanding stretching cylinder, Chin. Phys. Lett. 28 (12) (2011) 124707-1-4.
 [13] T. Fang, S. Yao, Viscous swirling flow over a stretching cylinder, Chin. Phys. Lett. 28 (11) (2011) 114702-1-4.
 [14] C. Y. Wang, Natural convection on a vertical stretching cylinder, Commun. Nonlinear Sci. Numer. Simulat, 17 (2012) 1098-1103.

- [15] B. J. Gireesha, B. Mahanthesh, P. T. Manjunatha, R. S. R. Gorla, Numerical solution for hydromagnetic boundary layer flow and heat transfer past a stretching surface embedded in non-Darcy porous medium with fluid-particle suspension, *J. Nigerian Math. Society*, doi:10.1016/j.jnnms.2015.07.003.
- [16] S. Mukhopadhyay, MHD boundary layer slip flow along a stretching cylinder, *Ain Shams Eng. J.* 4(2) (2013) 317-324.
- [17] Abdul Rehman, S. Nadeem, Heat Transfer Analysis of the Boundary Layer Flow over a Vertical Exponentially Stretching Cylinder, *Global J. Sci. Frontier Res. Math. Decision Sci.* 13(11) (2013) 73-85.
- [18] Abdul Rehman, S. Nadeem, S. Iqbal, M. Y. Malik, M. Naseer, Nanoparticle effect over the boundary layer flow over an exponentially stretching cylinder, *Proc IMechE Part N: J Nanoengineering and Nanosystems*, (2014) 1-6.
- [19] M. Naseer, M. Y. Malik, Abdul Rehman, Numerical Study of Convective Heat Transfer on the Power Law Fluid over a Vertical Exponentially Stretching Cylinder, *Applied and Comp.Math.* 4(5) (2015) 346-350.
- [20] X. Si, Lin Li, L. Zheng, X. Zhang, B. Liu, The exterior unsteady viscous flow and heat transfer due to a porous expanding stretching cylinder, *Computers & Fluids*, 105(10) (2014) 280-284.
- [21] K. Vajravelu, K. V. Prasad, S. R. Santhi, Axisymmetric magneto-hydrodynamic (MHD) flow and heat transfer at a non-isothermal stretching cylinder, *App. Math. Comp.* 219(8) (2012) 3993-4005.
- [22] H. B. Keller, Numerical methods in boundary layer theory, *Annu. Rev. Fluid Mech.* 10 (1978) 417-433.
- [23] T. Cebeci, P. Bradshaw, *Physical and Computational Aspects of Convective Heat Transfer*, springer-Verlag, New York, 1984.
- [24] S. Nadeem, Abdul Rehman, M. Y. Malik, Boundary layer stagnation-point flow of third grade fluid over an exponentially stretching sheet, *Braz. Soci. Che. Eng.* in press.
- [25] M. E. Ali, Heat transfer characteristics of a continuous stretching surface, *Warme und Stoubertagung* 29 (1994) 227-234.